Parviz Malekzadeh and Mohammad Shojaee*

A unified formulation for free vibration of functionally graded plates

DOI 10.1515/secm-2016-0031
Received February 1, 2016; accepted May 7, 2016; previously published online September 17, 2016

Abstract: A simple, accurate, and unified formulation for the free vibration analysis of functionally graded (FG) plates is introduced. New four-variable first-order and higher-order shear deformation theories together with the classical FG plate theory can be easily achieved. The only assumption is that the transverse displacement consists of bending and shear components, and hence the theory has the potential to be used for modeling of the nonlinear FG plate problems. To validate the proposed formulation, the free vibration analysis of FG plates on two-parameter elastic foundation is conducted. The material properties vary continuously through the plate thickness. Analytical solutions for simply supported and approximate solutions for FG plates with arbitrary boundary conditions are extracted by extending the application of the conventional differential quadrature method as an accurate and efficient numerical tool. Comparison studies with existing two- and three-dimensional results available in open literature are performed. Excellent agreement between the results of the present formulation and the other theories is observed.

Keywords: analytical modeling; functionally graded materials; numerical analysis; plates; vibration.

1 Introduction

Because of their superior thermomechanical properties, functionally graded materials (FGMs) have received wide applications as structural components in modern industries such as mechanical, aerospace, nuclear, reactors, and civil engineering in recent years [1]. Hence, significant efforts have been devoted to study the mechanical behaviors of structural elements made of these materials such as beams, plates, and shells. Also, it is well known that the vibration characteristic of plates made of FGMs is of great interest for better applications, engineering design, and manufacture.

Even if there are different two-dimensional theories for the free vibration analysis of functionally graded (FG) plates such as the classical plate theory (CPT) [2, 3], the first-order shear deformation theory (FSDT) [4–11], and the higher-order shear deformation theory (HSDT) [12–30], however, simple and accurate theories with low computational calculations can be still useful for both practical applications and theoretical studies on the free vibration of FG plates.

Because the transverse shear deformation effects are neglected in the CPT, it provides reasonable results for thin plates. For moderately thick plates, it underestimates deflection and overestimates buckling load as well as natural frequency [2, 3]. To overcome the deficiency of the CPT, many shear deformation theories have been used for the free vibration analysis of FG rectangular plates [12–30]. The basic idea of these theories is based on the explanation of the in-plane and out-of-plane (transverse) displacement components in terms of known functions of the material coordinate in the plate thickness direction with unknown coefficients. The unknown coefficients are only functions of the in-plane material coordinate variables, and hence, the three-dimensional elasticity theory reduces to a two-dimensional theory one. In most of these theories, the polynomial series expansion is used [12–24]. However, other functions such as hyperbolic functions [25, 26] or trigonometric functions [27] have been used by some researchers.

The simplest theory based on the polynomial series expansion is the FSDT. On the basis of this theory, only the linear terms in the series expansion of the in-plane displacement components are considered, and the transverse displacement is assumed to be constant through the thickness. According to these assumptions, the transverse shear stresses become constant through the thickness, but this assumption violates the shear stress-free surface conditions. Hence, shear correction factors are used to compensate for the difference between the actual stress state and the constant stress state [4–11]. To avoid the use of

***Corresponding author: Mohammad Shojaee,** Department of Mechanical and Aerospace Engineering, Shiraz University of Technology, Shiraz, Iran, e-mail: m.shojaee4@yahoo.com; m.shojaee@sutech.ac.ir
Parviz Malekzadeh: Department of Mechanical Engineering, School of Engineering, Persian Gulf University, Bushehr, Iran

shear correction factor, usually, the higher-order terms in the series expansions are considered [12–24]. Depending on the numbers of terms in the in-plane displacement components expansion, whether the transverse displacement is assumed to be constant, whether stress-free boundary conditions are satisfied (constraint theory) or not (unconstraint theory), and whether additional assumptions are used to obtain the unknown coefficients, different HSDTs have been developed [12–30].

Reddy's third-order shear deformation theory [31], which has been initially developed for laminated composite plates, has been used by some researchers to study the free vibration of the FG rectangular plates [12–15]. On the basis of this theory, the stress-free conditions on the top and bottom surface of the plate are satisfied by the displacement components (constraint theory).

Some others used unconstraint shear deformation theories. Roque et al. [16] and Shahrjerdi [17] developed unconstraint third- and second-order shear deformation theories for the free vibration analysis of FG plates, respectively. In both theories, constant transverse displacement was assumed.

To reduce the number of unknown variables, Benachour et al. [18] and Mechab et al. [19] extended the two-variable third-order shear deformation theory of Shimpi [32] to develop the four-variable third-order shear deformation theories for the free vibration of FG plates. The work of Malekzadeh et al. [33] differs from the others for its functions adopted in the in-plane displacement explanation.

Usually, the thickness stretching of the FG plates has been disregarded by neglecting the variation of the transverse displacement component along the thickness direction [12–19, 25]. However, in some studies, the polynomial series expansion has been used for this displacement component in the thickness direction [20–24, 26, 27]. Qian et al. [20, 21] applied a higher-order shear and normal deformable plate theory to analyze the static, free, and forced vibrations of a thick rectangular FG plates. On the basis of this theory, the three components of displacement were expanded in terms of Legendre polynomials in the thickness direction. Matsunaga [22] presented a two-dimensional higher-order deformation theory for the free vibration and stability analysis of FG plates. The in-plane and the transverse displacement components were expressed as polynomial power series of the thickness coordinate variable. Fares et al. [23] developed a two-dimensional theory account for the displacements field in which the in-plane displacements vary linearly through the plate thickness, whereas the out-of-plane displacement was a quadratic function of the thickness coordinate variable. Talha and Singh [24] proposed a third-order shear deformation theory, which included the quadratic variation of the transverse displacement through the plate thickness to study the free vibration of FG rectangular plates.

In the previously reviewed studies, the in-plane displacement components have been expanded in terms of the polynomial functions of the thickness coordinate variable. Ait Atmane [25] used the hyperbolic functions to represent through the thickness variation of the in-plane displacement components and implement the stress-free boundary conditions on the top and the bottom of the FG plates. Neves et al. [26, 27] presented sinusoidal and hyperbolic shear deformation theories for the static and free vibration analysis of FG plates by assuming sinusoidal and hyperbolic type variations across the thickness coordinate for the in-plane displacement components, respectively. In both theories, a quadratic variation was considered for the transverse displacement component in the thickness direction.

The aim of this work is to represent a simple, accurate, and unified formulation for the free vibration analysis of FG plates. New four-variable first- and third-order shear deformation theories, as against five variables in the case of the conventional form of these theories, and also CPT are easily achieved. This theory is free of the assumption of zero in-plane resultant forces used in developing the other four-variable shear deformation theories [18, 19, 34] and hence has the potential to be used for modeling of the nonlinear FG plate problems. In addition, despite the other four-variable theories [18, 19, 34], only the transverse displacement is assumed to consist of bending and shear components. As a result, some new functions are created for the in-plane displacement component explanation. The in-plane displacements cause the parabolic variations of shear strains through the thickness in such a way that the transverse shear stresses vanish on the top and bottom plate surfaces. The theory takes into account the quadratic variation of the transverse shear strains through the thickness of the plate, and hence, it does not require the use of shear correction factors. The equations of motion and the related boundary conditions for the FG plates on two-parameter elastic foundation are derived using Hamilton's principle. Exact solutions for the simply supported FG plates are extracted. In addition, by extending the application of differential quadrature method (DQM) as an accurate and computationally efficient numerical method [9, 33–38], approximate solutions for the FG plates with arbitrary boundary conditions are developed. Comparison studies with the other available two- and three-dimensional solutions in the open literature are performed, and excellent agreement is observed.

2 Theoretical formulation

Consider an FG rectangular plate of length $L_x = a$, width $L_y = b$, and thickness h, which is supported on a two-parameter elastic foundation as shown in Figure 1. A Cartesian coordinate system (x, y, z) is used to label the material points of the plates in the undeformed reference configuration. The in-plane displacement components $\bar{u}$ (in the x-direction) and $\bar{v}$ (in the y-direction) and the transverse displacement component $\bar{w}$ (in the z-direction) can be approximated as

$$\bar{u}(x, y, z, t) = u(x, y, t) + z\varphi_1 + z^2\varphi_2 + z^3\varphi_3, \tag{1a}$$

$$\bar{v}(x, y, z, t) = v(x, y, t) + z\psi_1 + z^2\psi_2 + z^3\psi_3, \tag{1b}$$

$$\bar{w}(x, y, z, t) = w^b(x, y, t) + w^s(x, y, t), \tag{1c}$$

where u and v are the in-plane displacement components of material points on the mid-plane of the FG plate along the x- and y-directions, respectively, and w^b and w^s are the bending and shear transverse displacement components of an arbitrary material point of the FG plate. In addition, φ_i and ψ_i (with $i = 1, 2, 3$) are functions that represent the thickness variations of the in-plane displacement components.

In this study, as a first assumption, the functions due to the linear variation of the in-plane displacement components are approximated as

$$\varphi_1 = -\frac{\partial w^b}{\partial x}, \tag{2a}$$

$$\psi_1 = -\frac{\partial w^b}{\partial y}. \tag{2b}$$

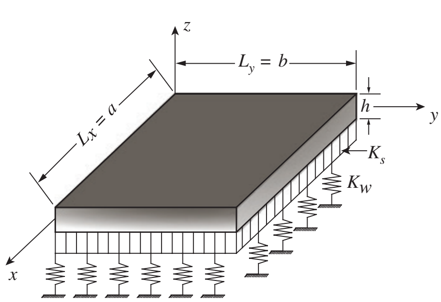

Figure 1: The FG plate supported on elastic foundation.

This assumption together with the zero shear stress components on the top and bottom surface of the FG plate can easily reduce the theory to the CPT one. For an isotropic FG plate, the last aforementioned assumption gives

$$\gamma_{xz} = 0, \tag{3a}$$

$$\gamma_{yz} = 0 \text{ at } z = \pm h/2, \tag{3b}$$

where γ_{iz} (with $i = x, y$) are the transverse shear strain components. On the basis of the linear elasticity theory, Equations (1), (2), and (3) yield

$$\varphi_2 = 0, \tag{4a}$$

$$\psi_2 = 0, \tag{4b}$$

$$\varphi_3 = -\alpha\frac{\partial w^s}{\partial x}, \tag{4c}$$

$$\psi_3 = -\alpha\frac{\partial w^s}{\partial y}, \tag{4d}$$

where $\alpha = \frac{4}{3h^2}$. Using Equations (1), (2), and (4), the nonzero linear strain tensor components in terms of displacement components become

$$\varepsilon_{xx} = \frac{\partial u}{\partial x} - z\frac{\partial^2 w^b}{\partial x^2} - \alpha z^3\frac{\partial^2 w^s}{\partial x^2}, \tag{5a}$$

$$\varepsilon_{yy} = \frac{\partial v}{\partial y} - z\frac{\partial^2 w^b}{\partial y^2} - \alpha z^3\frac{\partial^2 w^s}{\partial y^2}, \tag{5b}$$

$$\gamma_{xy} = \frac{\partial v}{\partial x} + \frac{\partial u}{\partial y} - 2z\frac{\partial^2 w^b}{\partial x\partial y} - 2\alpha z^3\frac{\partial^2 w^s}{\partial x\partial y}, \tag{5c}$$

$$\gamma_{yz} = (1 - 3\alpha z^2)\frac{\partial w^s}{\partial y}, \tag{5d}$$

$$\gamma_{xz} = (1 - 3\alpha z^2)\frac{\partial w^s}{\partial x}, \tag{5e}$$

where ε_{ii} (with $i = x, y$) and γ_{xy} are the in-plane normal and shear strain tensor components, respectively.

It is interesting to note that if one insert $\alpha = 0$ in the strain tensor components, the theory reduces to a new first-order shear deformation theory (NFSDT), which has four degrees of freedom instead of five degrees of freedom of the conventional FSDT. The strain components of this new FSDT become

$$\varepsilon_{xx} = \frac{\partial u}{\partial x} - z\frac{\partial^2 w^b}{\partial x^2}, \tag{6a}$$

$$\varepsilon_{yy}=\frac{\partial v}{\partial y}-z\frac{\partial^2 w^b}{\partial y^2},\tag{6b}$$

$$\gamma_{xy}=\frac{\partial v}{\partial x}+\frac{\partial u}{\partial y}-2z\frac{\partial^2 w^b}{\partial x\partial y},\tag{6c}$$

$$\gamma_{xz}=\frac{\partial w^s}{\partial x},\tag{6d}$$

$$\gamma_{yz}=\frac{\partial w^s}{\partial y}.\tag{6e}$$

In addition, if the shear component of the transverse displacement is neglected, then the theory reduces to the CPT one, which has the following nonzero strain components:

$$\varepsilon_{xx}=\frac{\partial u}{\partial x}-z\frac{\partial^2 w^b}{\partial x^2},\tag{7a}$$

$$\varepsilon_{yy}=\frac{\partial v}{\partial y}-z\frac{\partial^2 w^b}{\partial y^2},\tag{7b}$$

$$\gamma_{xy}=\frac{\partial v}{\partial x}+\frac{\partial u}{\partial y}-2z\frac{\partial^2 w^b}{\partial x\partial y}.\tag{7c}$$

According to the linear elasticity theory and the present HSDT, the relation between the nonzero stress tensor components and the displacement components can be written as

$$\sigma_{xx}=\frac{E}{(1-\nu^2)}\left[\frac{\partial u}{\partial x}+\nu\frac{\partial v}{\partial y}-z\left(\frac{\partial^2 w^b}{\partial x^2}+\nu\frac{\partial^2 w^b}{\partial y^2}\right)-\alpha z^3\left(\frac{\partial^2 w^s}{\partial x^2}+\nu\frac{\partial^2 w^s}{\partial y^2}\right)\right],\tag{8a}$$

$$\sigma_{yy}=\frac{E}{(1-\nu^2)}\left[\frac{\partial v}{\partial y}+\nu\frac{\partial u}{\partial x}-z\left(\frac{\partial^2 w^b}{\partial y^2}+\nu\frac{\partial^2 w^b}{\partial y^2}\right)-\alpha z^3\left(\frac{\partial^2 w^s}{\partial y^2}+\nu\frac{\partial^2 w^s}{\partial x^2}\right)\right],\tag{8b}$$

$$\sigma_{xy}=G\left[\frac{\partial u}{\partial y}+\frac{\partial v}{\partial x}-2z\left(\frac{\partial^2 w^b}{\partial x\partial y}\right)-2\alpha z^3\frac{\partial^2 w^s}{\partial x\partial y}\right],\tag{8c}$$

$$\sigma_{xz}=G(1-3\alpha z^2)\frac{\partial w^s}{\partial x},\tag{8d}$$

$$\sigma_{yz}=G(1-3\alpha z^2)\frac{\partial w^s}{\partial y},\tag{8e}$$

where E, $G\left[=\frac{E}{2(1+\nu)}\right]$, and ν are Young's modulus, shear rigidity, and Poisson's ratio of the FG plate, respectively. Also, the material properties of the plate are assumed to vary continuously through the thickness of the plate. In this study, an arbitrary material property P of the FG plate is obtained by using the power law distribution as

$$P(z)=P_{\mathrm{m}}+[P_{\mathrm{c}}-P_{\mathrm{m}}](V_{\mathrm{f}})^p,\ p\geq 0\tag{9}$$

where the subscripts c and m refer to the ceramic and metal constituents, respectively; p is the material property graded index or the power law index; and $V_{\mathrm{f}}\left[=\left(\frac{2z+h}{2h}\right)\right]$ is the volume fraction [39–45].

The equations of motion and the related boundary conditions can be derived in a systematic manner using Hamilton's principle, which for the free vibration analysis takes the following form:

$$\int_{t_1}^{t_2}(\delta K-\delta U)dt=0,\tag{10}$$

where δK and δU are the variation of the kinetic energy and strain energy, respectively, and t_1 and t_2 are two arbitrary times.

The variation of strain energy of the FG plate can be stated as

$$\begin{aligned}\delta U=&\int_V\left\{\sigma_{xx}\left(\frac{\partial\delta u}{\partial x}-z\frac{\partial^2\delta w^b}{\partial x^2}-\alpha z^3\frac{\partial^2\delta w^s}{\partial x^2}\right)+\sigma_{yy}\left(\frac{\partial v}{\partial y}-z\frac{\partial^2 w^b}{\partial y^2}\right.\right.\\&\left.-\alpha z^3\frac{\partial^2 w^s}{\partial y^2}\right)+\sigma_{xy}\left(\frac{\partial\delta v}{\partial x}+\frac{\partial\delta u}{\partial y}-2z\frac{\partial^2\delta w^b}{\partial x\partial y}-2\alpha z^3\frac{\partial^2\delta w^s}{\partial x\partial y}\right)\\&\left.+\sigma_{xz}(1-3\alpha z^2)\frac{\partial\delta w^s}{\partial x}+\sigma_{yz}(1-3\alpha z^2)\frac{\partial\delta w^s}{\partial y}\right\}dV\\&+\int_A\left\{k_{\mathrm{s}}\left[\frac{\partial(w^b+w^s)}{\partial x}\frac{\partial(\delta w^b+\delta w^s)}{\partial x}+\frac{\partial(w^b+w^s)}{\partial y}\frac{\partial(\delta w^b+\delta w^s)}{\partial y}\right]\right.\\&\left.+k_{\mathrm{w}}(w^b+w^s)(\delta w^b+\delta w^s)\right\}dA,\end{aligned}\tag{11}$$

where k_w (N/m³) is the spring or Winkler parameter of the elastic foundation and k_s (N/m) is the shear or Pasternak parameter of the elastic foundation, which are shown in Figure 1 [46–48]. Also, the variation of kinetic energy is obtained as

$$\begin{aligned}\delta T=&\int_V\left(\frac{\partial\bar{u}}{\partial t}\frac{\partial\delta\bar{u}}{\partial t}+\frac{\partial\bar{v}}{\partial t}\frac{\partial\delta\bar{v}}{\partial t}+\frac{\partial w}{\partial t}\frac{\partial\delta w}{\partial t}\right)\\=&\int_V\left[\left(\frac{\partial u}{\partial t}-z\frac{\partial w^b}{\partial t\partial x}-\alpha z^3\frac{\partial w^s}{\partial t\partial x}\right)\left(\frac{\partial\delta u}{\partial t}-z\frac{\partial\delta w^b}{\partial t\partial x}-\alpha z^3\frac{\partial\delta w^s}{\partial t\partial x}\right)\right.\\&+\left(\frac{\partial v}{\partial t}-z\frac{\partial w^b}{\partial t\partial y}-\alpha z^3\frac{\partial w^s}{\partial t\partial y}\right)\left(\frac{\partial\delta v}{\partial t}-z\frac{\partial\delta w^b}{\partial t\partial y}-\alpha z^3\frac{\partial\delta w^s}{\partial t\partial y}\right)\\&\left.+\frac{\partial(w^b+w^s)}{\partial t}\frac{\partial(\delta w^b+\delta w^s)}{\partial t}\right]dV.\end{aligned}\tag{12}$$

Substituting Equations (11) and (12) into Equation (10) and performing the integration by parts, the equations of motion and the related boundary conditions of the proposed plate theory are obtained as follows:

δu:

$$\frac{\partial N_{xx}}{\partial x}+\frac{\partial N_{xy}}{\partial y}=I_0\frac{\partial^2 u}{\partial t^2}-I_1\frac{\partial^3 w^b}{\partial t^2\partial x}-\alpha I_3\frac{\partial^3 w^s}{\partial t^2\partial x} \quad (13)$$

δv:

$$\frac{\partial N_{yy}}{\partial y}+\frac{\partial N_{xy}}{\partial x}=I_0\frac{\partial^2 v}{\partial t^2}-I_1\frac{\partial^3 w^b}{\partial t^2\partial y}-\alpha I_3\frac{\partial^3 w^s}{\partial t^2\partial y} \quad (14)$$

δw_b:

$$\frac{\partial^2 M_{xx}}{\partial x^2}+2\frac{\partial^2 M_{xy}}{\partial x\partial y}+\frac{\partial^2 M_{yy}}{\partial y^2}-k_w(w^b+w^s)$$
$$+k_s\nabla^2(w^b+w^s)=I_0\frac{\partial^2(w^b+w^s)}{\partial t^2}$$
$$+I_1\frac{\partial^2}{\partial t^2}\left(\frac{\partial u}{\partial x}+\frac{\partial v}{\partial y}\right)-I_2\frac{\partial^2}{\partial t^2}(\nabla^2 w^b)-\alpha I_4\frac{\partial^2}{\partial t^2}(\nabla^2 w^s) \quad (15)$$

δw_s:

$$\alpha\left(\frac{\partial^2 P_{xx}}{\partial x^2}+2\frac{\partial^2 P_{xy}}{\partial x\partial y}+\frac{\partial^2 P_{yy}}{\partial y^2}\right)+\frac{\partial Q_x}{\partial x}+\frac{\partial Q_y}{\partial y}-k_w(w^b+w^s)$$
$$+k_s\nabla^2(w^b+w^s)=I_0\frac{\partial^2(w^b+w^s)}{\partial t^2}+\alpha I_3\frac{\partial^2}{\partial t^2}\left(\frac{\partial u}{\partial x}+\frac{\partial v}{\partial y}\right)$$
$$-\alpha I_4\frac{\partial^2}{\partial t^2}(\nabla^2 w^b)-\alpha^2 I_6\frac{\partial^2}{\partial t^2}(\nabla^2 w^s) \quad (16)$$

In-plane boundary conditions:

Either $u_n=n_x u+n_y v$ is prescribed or

$$N_{nn}=n_x^2 N_{xx}+n_x n_y N_{xy}+n_y^2 N_{yy}=0. \quad (17a, b)$$

Either $u_s=-n_y u+n_x v$ is prescribed or

$$N_{ns}=(n_x^2-n_y^2)N_{xy}-n_x n_y(N_{yy}-N_{xx})=0. \quad (18a, b)$$

Out-of-plane boundary conditions:

Either w^b is prescribed or

$$V_n^b=\left(\frac{\partial M_{xx}}{\partial x}+\frac{\partial M_{xy}}{\partial y}\right)n_x+\left(\frac{\partial M_{yy}}{\partial y}+\frac{\partial M_{xy}}{\partial x}\right)n_y$$
$$+k_s\frac{\partial(w^b+w^s)}{\partial n}=0. \quad (19a, b)$$

Either $\frac{\partial w^b}{\partial n}$ is prescribed or

$$M_{nn}=n_x^2 M_{xx}+n_x n_y M_{xy}+n_y^2 M_{yy}=0. \quad (20a, b)$$

Either w^s is prescribed or

$$V_n^s=\left(\frac{\partial P_{xx}}{\partial x}+\frac{\partial P_{xy}}{\partial y}\right)n_x+\left(\frac{\partial P_{yy}}{\partial y}+\frac{\partial P_{xy}}{\partial x}\right)n_y$$
$$+Q_x n_x+Q_y n_y+k_s\frac{\partial(w^b+w^s)}{\partial n}=0. \quad (21a, b)$$

Either $\frac{\partial w^s}{\partial n}$ is prescribed or

$$P_{nn}=n_x^2 P_{xx}+n_x n_y P_{xy}+n_y^2 P_{yy}=0, \quad (22a, b)$$

where $\frac{\partial(\ )}{\partial n}=n_x\frac{\partial(\ )}{\partial x}+n_y\frac{\partial(\ )}{\partial y}$; N_{ij}, M_{ij}, P_{ij}, and Q_i with $(i, j=x, y)$ are the stress resultants, and I_i $(i=0, 1, \ldots, 4, 6)$ is the mass inertia, which has the following definitions:

$$(N_{ij}, M_{ij}, P_{ij})=\int_{-\frac{h}{2}}^{\frac{h}{2}}(1, z, z^3)\sigma_{ij}dz, \quad (23a)$$

$$Q_i=\int_{-\frac{h}{2}}^{\frac{h}{2}}(1-3\alpha z^2)\sigma_{iz}dz, \quad (23b)$$

$$I_i=\int_{-\frac{h}{2}}^{\frac{h}{2}}\rho z^i dz, \quad (23c)$$

where ρ is the mass density of the FG plate. Substituting for the stress tensor components in terms of the displacement components from Equation (8), one obtains

$$\begin{Bmatrix} N_{xy}\\ M_{xy}\\ P_{xy}\end{Bmatrix}=\begin{bmatrix} A_s & B_s & \alpha C_s\\ B_s & D_s & \alpha F_s\\ C_s & F_s & \alpha H_s\end{bmatrix}\begin{Bmatrix}\frac{\partial u}{\partial y}+\frac{\partial v}{\partial x}\\ -2\frac{\partial^2 w^b}{\partial x\partial y}\\ -2\frac{\partial^2 w^s}{\partial x\partial y}\end{Bmatrix}, \quad (24a)$$

$$\begin{Bmatrix} Q_x\\ Q_y\end{Bmatrix}=\begin{bmatrix} D_s^i & 0\\ 0 & D_s^i\end{bmatrix}\begin{Bmatrix}\frac{\partial w^s}{\partial x}\\ \frac{\partial w^s}{\partial y}\end{Bmatrix}, \quad (24b)$$

$$\begin{Bmatrix} N_{xx}\\ N_{yy}\\ M_{xx}\\ M_{yy}\\ P_{xx}\\ P_{yy}\end{Bmatrix}=\begin{bmatrix} A & \hat{A} & B & \hat{B} & \alpha C & \alpha\hat{C}\\ \hat{A} & A & \hat{B} & B & \alpha\hat{C} & \alpha C\\ B & \hat{B} & D & \hat{D} & \alpha F & \alpha\hat{F}\\ \hat{B} & B & \hat{D} & D & \alpha\hat{F} & \alpha F\\ C & \hat{C} & F & \hat{F} & \alpha H & \alpha\hat{H}\\ \hat{C} & C & \hat{F} & F & \alpha\hat{H} & \alpha H\end{bmatrix}\begin{Bmatrix}\frac{\partial u}{\partial x}\\ \frac{\partial v}{\partial y}\\ -\frac{\partial^2 w^b}{\partial x^2}\\ -\frac{\partial^2 w^b}{\partial y^2}\\ -\frac{\partial^2 w^s}{\partial x^2}\\ -\frac{\partial^2 w^s}{\partial y^2}\end{Bmatrix}, \quad (24c)$$

where the stiffness coefficients are

$$\begin{bmatrix} A & B & D & C & F & H \\ \hat{A} & \hat{B} & \hat{D} & \hat{C} & \hat{F} & \hat{H} \\ A_s & B_s & D_s & C_s & F_s & H_s \end{bmatrix} = \int_{-\frac{h}{2}}^{\frac{h}{2}} \begin{bmatrix} \hat{E}(z) \\ \nu\hat{E}(z) \\ G(z) \end{bmatrix} [1 \quad z \quad z^2 \quad z^3 \quad z^4 \quad z^6] dz,$$

$$\hat{E} = \frac{E}{(1-\nu^2)} \tag{25a}$$

$$D_s^i = \int_{-\frac{h}{2}}^{\frac{h}{2}} G(z)(1-3\alpha z^2)^2 dz. \tag{25b}$$

Different types of classical boundary conditions at the edges of the plate can be obtained by combining the conditions stated in Equations (17–22). Two types of boundary conditions that are considered in this study are as follows:

Simply support (S):

$$u_s = 0,\ w^b = 0,\ w^s = 0,\ N_{nn} = 0,\ M_{nn} = 0,\ P_{nn} = 0 \tag{26a–f}$$

Clamped (C):

$$u_n = 0,\ u_s = 0,\ w^b = 0,\ w^s = 0,\ \frac{\partial w^b}{\partial n} = 0,\ \frac{\partial w^s}{\partial n} = 0 \tag{27a–f}$$

Using Equations (8) and (23), the equations of motion [Equations (13–16)] in terms of the displacement components take the following forms, respectively:

Equation (13):

$$A\frac{\partial^2 u}{\partial x^2} + \hat{A}\frac{\partial^2 v}{\partial x \partial y} - B\frac{\partial^3 w^b}{\partial x^3} - \hat{B}\frac{\partial^3 w^b}{\partial x \partial y^2} - \alpha C\frac{\partial^3 w^s}{\partial x^3} - \alpha\hat{C}\frac{\partial^3 w^s}{\partial x \partial y^2} + A_s\left(\frac{\partial^2 u}{\partial y^2} + \frac{\partial^2 v}{\partial x \partial y}\right) - 2B_s\frac{\partial^3 w^b}{\partial x \partial y^2} - 2\alpha C_s\frac{\partial^3 w^s}{\partial x \partial y^2} = I_0\frac{\partial^2 u}{\partial t^2} - I_1\frac{\partial^3 w^b}{\partial t^2 \partial x} - \alpha I_3\frac{\partial^3 w^s}{\partial t^2 \partial x} \tag{28}$$

Equation (14):

$$A\frac{\partial^2 v}{\partial y^2} + \hat{A}\frac{\partial^2 u}{\partial x \partial y} - B\frac{\partial^3 w^b}{\partial y^3} - \hat{B}\frac{\partial^3 w^b}{\partial y \partial x^2} - \alpha C\frac{\partial^3 w^s}{\partial y^3} - \alpha\hat{C}\frac{\partial^3 w^s}{\partial y \partial x^2} + A_s\left(\frac{\partial^2 u}{\partial x \partial y} + \frac{\partial^2 v}{\partial x^2}\right) - 2B_s\frac{\partial^3 w^b}{\partial y \partial x^2} - 2\alpha C_s\frac{\partial^3 w^s}{\partial y \partial x^2} = I_0\frac{\partial^2 v}{\partial t^2} - I_1\frac{\partial^3 w^b}{\partial t^2 \partial y} - \alpha I_3\frac{\partial^3 w^s}{\partial t^2 \partial y} \tag{29}$$

Equation (15):

$$B\frac{\partial^3 u}{\partial x^3} + \hat{B}\frac{\partial^3 v}{\partial x^2 \partial y} - D\frac{\partial^4 w^b}{\partial x^4} - \hat{D}\frac{\partial^4 w^b}{\partial x^2 \partial y^2} - \alpha F\frac{\partial^4 w^s}{\partial x^4} - \alpha\hat{F}\frac{\partial^4 w^s}{\partial x^2 \partial y^2} + 2B_s\left(\frac{\partial^3 u}{\partial y^2 \partial x} + \frac{\partial^3 v}{\partial x^2 \partial y}\right) - 4D_s\frac{\partial^4 w^b}{\partial x^2 \partial y^2} - 4\alpha F_s\frac{\partial^4 w^s}{\partial x^2 \partial y^2} + \hat{B}\frac{\partial^3 u}{\partial y^2 \partial x} + B\frac{\partial^3 v}{\partial y^3} - D\frac{\partial^4 w^b}{\partial y^4} - \hat{D}\frac{\partial^4 w^b}{\partial x^2 \partial y^2} - \alpha F\frac{\partial^4 w^s}{\partial y^4} - \alpha\hat{F}\frac{\partial^4 w^s}{\partial x^2 \partial y^2} - k_w(w^b + w^s) + k_s\nabla^2(w^b + w^s) = I_0\frac{\partial^2(w^b + w^s)}{\partial t^2} + I_1\frac{\partial^2}{\partial t^2}\left(\frac{\partial u}{\partial x} + \frac{\partial v}{\partial y}\right) - I_2\frac{\partial^2}{\partial t^2}(\nabla^2 w^b) - \alpha I_4\frac{\partial^2}{\partial t^2}(\nabla^2 w^s) \tag{30}$$

Equation (16):

$$\alpha\left[C\frac{\partial^3 u}{\partial x^3} + \hat{C}\frac{\partial^3 v}{\partial x^2 \partial y} - F\frac{\partial^4 w^b}{\partial x^4} - \hat{F}\frac{\partial^4 w^b}{\partial x^2 \partial y^2} - \alpha H\frac{\partial^4 w^s}{\partial x^4} - \alpha\hat{H}\frac{\partial^4 w^b}{\partial x^2 \partial y^2} + 2C_s\left(\frac{\partial u}{\partial y^2 \partial x} + \frac{\partial v}{\partial x^2 \partial y}\right) - 4F_s\frac{\partial^4 w^b}{\partial x^2 \partial y^2} - 4\alpha H_s\frac{\partial^4 w^s}{\partial x^2 \partial y^2} + B\frac{\partial^3 u}{\partial y^2 \partial x} + \hat{B}\frac{\partial^3 v}{\partial y^3} - F\frac{\partial^4 w^b}{\partial y^4} - \hat{F}\frac{\partial^4 w^b}{\partial x^2 \partial y^2} - \alpha H\frac{\partial^4 w^s}{\partial y^4} - \alpha\hat{H}\frac{\partial^4 w^s}{\partial x^2 \partial y^2}\right] + D_s^i\nabla^2 w^s - k_w(w^b + w^s) + k_s\nabla^2(w^b + w^s) = I_0\frac{\partial(w^b + w^s)}{\partial t^2} - \alpha^2 I_6\frac{\partial^2}{\partial t^2}(\nabla^2 w^s) + \alpha I_3\frac{\partial^2}{\partial t^2}\left(\frac{\partial u}{\partial x} + \frac{\partial v}{\partial y}\right) - \alpha I_4\frac{\partial^2}{\partial t^2}(\nabla^2 w^b) \tag{31}$$

In a similar manner, the natural boundary conditions can be expressed in terms of the displacement components.

3 Solution procedure

3.1 Analytical solution for the simply supported FG plates

For the simply supported FG plates, the displacement components can be represented in the following forms, which automatically satisfy the related conditions at the edges of the FG plates:

$$u(x,\ y,\ t) = \sum_{m=1}^{\infty}\sum_{n=1}^{\infty} U_{mn} e^{J\omega_{mn} t} \cos\beta_m x \sin\gamma_n y, \tag{32a}$$

$$v(x,\ y,\ t) = \sum_{m=1}^{\infty}\sum_{n=1}^{\infty} V_{mn} e^{J\omega_{mn} t} \sin\beta_m x \cos\gamma_n y, \tag{32b}$$

$$w^b(x, y, t)=\sum_{m=1}^{\infty}\sum_{n=1}^{\infty}W_{mn}^b e^{J\omega_{mn}t}\sin\beta_m x\sin\gamma_n y, \tag{32c}$$

$$w^s(x, y, t)=\sum_{m=1}^{\infty}\sum_{n=1}^{\infty}W_{mn}^s e^{J\omega_{mn}t}\sin\beta_m x\sin\gamma_n y, \tag{32d}$$

where $J=\sqrt{-1}$, $\beta_m=\dfrac{m\pi}{a}$, and $\gamma_n=\dfrac{n\pi}{b}$; m and n are the wave numbers along the x- and y-directions, respectively; U_{mn}, V_{mn}, W_{mn}^b, and W_{mn}^s are the amplitudes of the displacement components; and ω_{mn} is the natural frequency.

Inserting for the displacement components from Equation (32) into the equations of motion [Equations (28–31)], one obtains

$$([\hat{S}_{ij}^{mn}]-\omega_{mn}^2[\hat{M}_{ij}^{mn}])\{D_{mn}\}=0, \tag{33}$$

where $\{D_{mn}\}=\begin{Bmatrix} U_{mn} \\ V_{mn} \\ W_{mn}^b \\ W_{mn}^s \end{Bmatrix}$ is the vector of degrees of freedom; also, both the stiffness matrix $[\hat{S}_{ij}^{mn}]$ and the mass matrix $[\hat{M}_{ij}^{mn}]$ are symmetric, and their elements are

$$\hat{S}_{11}^{mn}=-(A\beta_m^2+A_s\gamma_n^2), \tag{34a}$$

$$\hat{S}_{12}^{mn}=-(\hat{A}+A_s)\beta_m\gamma_n, \tag{34b}$$

$$\hat{S}_{13}^{mn}=-\beta_m[B\beta_m^2+(\hat{B}+2B_s)\gamma_n^2], \tag{34c}$$

$$\hat{S}_{14}^{mn}=-\alpha\beta_m[C\beta_m^2+(\hat{C}+2C_s)\gamma_n^2], \tag{34d}$$

$$\hat{S}_{22}^{mn}=-(A\gamma_m^2+A_s\beta_n^2), \tag{34e}$$

$$\hat{S}_{23}^{mn}=-\gamma_m[B\gamma_m^2+(\hat{B}+2B_s)\beta_n^2], \tag{34f}$$

$$\hat{S}_{24}^{mn}=-\alpha\gamma_m[C\gamma_m^2+(\hat{C}+2C_s)\beta_n^2], \tag{34g}$$

$$\hat{S}_{33}^{mn}=-[D\beta_m^4+2(\hat{D}+2D_s)\beta_n^2\gamma_n^2+D\gamma_n^4] -k_s(\beta_m^2+\gamma_n^2)-k_w, \tag{34h}$$

$$\hat{S}_{34}^{mn}=-\alpha[F\beta_m^4+2(\hat{F}+2F_s)\beta_n^2\gamma_n^2+F\gamma_n^4] -k_s(\beta_m^2+\gamma_n^2)-k_w, \tag{34i}$$

$$\hat{M}_{33}^{mn}=I_0+I_2(\beta_m^2+\gamma_n^2), \tag{34j}$$

$$\hat{S}_{44}^{mn}=-\alpha^2[H\beta_m^4+2(\hat{H}+2H_s)\beta_m^2\gamma_n^2+H\gamma_n^4] -k_s(\beta_m^2+\gamma_n^2)-k_w, \tag{34k}$$

$$\hat{M}_{13}^{mn}=-I_1\beta_m, \tag{34l}$$

$$\hat{M}_{14}^{mn}=-\alpha I_3\beta_m, \tag{34m}$$

$$\hat{M}_{23}^{mn}=-I_1\gamma_n, \tag{34n}$$

$$\hat{M}_{24}^{mn}=-\alpha I_3\gamma_n, \tag{34o}$$

$$\hat{M}_{34}^{mn}=I_0+\alpha I_4(\beta_m^2+\gamma_n^2), \tag{34p}$$

$$\hat{M}_{44}^{mn}=I_0+\alpha^2 I_6(\beta_m^2+\gamma_n^2). \tag{34q}$$

For the given values of the wave numbers m and n, the related natural frequencies are easily obtained from the system of algebraic eigenvalue equations [Equation (33)].

3.2 Approximate solution for the FG plates with arbitrary boundary conditions

Because it is difficult to obtain the analytical solution for the free vibration analysis of FG plates with arbitrary boundary conditions, the approximate methods should be used to solve the problem. On the other hand, the DQM is an efficient and accurate numerical approach in comparison with the weighted residual methods such as the finite element (FE) method [9, 33–38]. The weak form of the governing equations is solved in using the FE method, whereas the DQM discretizes the strong form of the governing equations. Furthermore, vice versa, the DQM exactly satisfies all types of boundary conditions. Also, the advantage of the DQM over the other meshless methods is its simplicity and low computational efforts [9, 33–38, 49, 50].

The basic idea of the DQM is that the derivatives of a function, with respect to a space variable at a given sampling point, are approximated as a weighted linear sum of the sampling points in the domain of that variable. In this method, at a given grid point (x_i, y_j), the first- and the second-order derivatives of a function can be approximated as

$$\left.\frac{\partial f}{\partial\eta}\right|_{(x_i,y_j)}=\sum_{m=1}^{N_\eta}A_{im}^{\eta}f_{mj}, \tag{35a}$$

$$\left.\frac{\partial^2 f}{\partial\eta^2}\right|_{(x_i,y_j)}=\sum_{m=1}^{N_\eta}B_{im}^{\eta}f_{mj}, \tag{35b}$$

for $i, j=1, \ldots, N_\eta$,

where $\eta = x$ or y; f_{ij} means the function value at the grid point (x_i, y_j); A^{η}_{im} and B^{η}_{im} are the weighting coefficients of the first- and second-order derivatives of the η-direction ($\eta = x$ or y), respectively; and N_η is the number of grid points along the η-direction ($\eta = x$ or y). To determine the weighting coefficients, a set of test functions should be used in Equation (35). For the polynomial basis functions DQM, a set of Lagrange polynomials are used as the test functions. The weighting coefficients for the first- and the second-order derivatives along the η-direction are determined as follows [33, 34, 38]:

$$A^{\eta}_{ij} = \begin{cases} \dfrac{1}{L_\eta} \dfrac{M(\eta_i)}{(\eta_i - \eta_j) M(\eta_j)} & \text{for } i \neq j \\ -\sum\limits_{\substack{i=1,\\ i\neq j}}^{N_\eta} A^{\eta}_{ij} & \text{for } i = j \text{ and } i, j = 1, 2\ldots, N_\eta \end{cases}, \qquad (36)$$

where $M(\eta_i) = \prod\limits_{\substack{j=1,\\ i\neq j}}^{N_\eta} (\eta_i - \eta_j)$ and L_η is the nanoplate length along the η-direction ($\eta = x$ or y). The weighting coefficients of the second-order derivative can be obtained as

$$[B^{\eta}_{ij}] = [A^{\eta}_{ij}][A^{\eta}_{ij}] = [A^{\eta}_{ij}]^2. \qquad (37)$$

It is shown that among the different rules for the grid generation, the Chebyshev-Gauss-Lobatto quadrature points give more accurate results [9, 33–38]. Hence, in this study, this type of grid generation rule is used.

One of the drawbacks of the conventional DQM is that the boundary condition imposition of the higher-order differential equations (order ≥ 3), which have multiple boundary conditions at a boundary grid points for a field variable, cannot be done in a straightforward manner. A special treatment is necessary to implement the multiple boundary conditions [34, 35]. To overcome this shortcoming, different methodologies have been suggested [34, 35]. In this work, the proposed approach by Karami and Malekzadeh [34] is further extended to implement the boundary conditions exactly at the boundary grid points. On the basis of this approach, the only degrees of freedom within the domain are the in-plane and transverse displacement components (u, v, w^b, w^s); however, along the boundaries, these displacement components as well as the second-order derivatives of the transverse displacement components (w^b, w^s) with respect to the associated normal coordinate variable to that boundary [34] are chosen as the degrees of freedom. Hence, along the edges $x = 0$ and a, the degrees of freedom become $\left(u, v, w^b, w^s, \dfrac{\partial^2 w^b}{\partial x^2}, \dfrac{\partial^2 w^s}{\partial x^2}\right)$, whereas along the edges $y = 0$ and b, these are $\left(u, v, w^b, w^s, \dfrac{\partial^2 w^b}{\partial y^2}, \dfrac{\partial^2 w^s}{\partial y^2}\right)$.

Using the differential quadrature (DQ) rules, the discretized form of Equations (28–31) are obtained as follows:

Equation (28):

$$\begin{aligned} & A\sum_{p=1}^{N_x} B^x_{ip} u_{pj} + \hat{A}\sum_{p=1}^{N_x}\sum_{q=1}^{N_y} A^x_{ip} A^y_{jq} v_{pq} - B\left(\sum_{p=1}^{N_x} \bar{C}^x_{ip} w^b_{pj} + A^x_{i1}\kappa^{xb}_{1j} + A^x_{iN_x}\kappa^{xb}_{N_x j}\right) \\ & - \hat{B}\sum_{p=1}^{N_x}\sum_{q=1}^{N_y} A^x_{ip} B^y_{jq} w^b_{pq} - \alpha C\left(\sum_{p=1}^{N_x} \bar{C}^x_{ip} w^s_{pj} + A^x_{i1}\kappa^{xs}_{1j} + A^x_{iN_x}\kappa^{xs}_{N_x j}\right) \\ & - \alpha\hat{C}\sum_{p=1}^{N_x}\sum_{q=1}^{N_y} A^x_{ip} B^y_{jq} w^s_{pq} - 2B_s\sum_{p=1}^{N_x}\sum_{q=1}^{N_y} A^x_{ip} B^y_{jq} w^b_{pq} \\ & + A_s\left(\sum_{q=1}^{N_y} B^y_{jq} u_{iq} + \sum_{p=1}^{N_x}\sum_{q=1}^{N_y} A^x_{ip} A^y_{jq} v_{pq}\right) - 2\alpha C_s\sum_{p=1}^{N_x}\sum_{q=1}^{N_y} A^x_{ip} B^y_{jq} w^s_{pq} \\ & = I_0\left(\frac{\partial^2 u}{\partial t^2}\right)_{ij} - I_1\sum_{p=1}^{N_x} A^x_{ip}\left(\frac{\partial^2 w^b}{\partial t^2}\right)_{pj} - I_3\sum_{p=1}^{N_x} A^x_{ip}\left(\frac{\partial^2 w^s}{\partial t^2}\right)_{pj} \end{aligned} \qquad (38)$$

Equation (29):

$$\begin{aligned} & A\sum_{q=1}^{N_y} B^y_{jq} v_{iq} + \hat{A}\sum_{p=1}^{N_x}\sum_{q=1}^{N_y} A^x_{ip} A^y_{jq} u_{pq} - B\left(\sum_{q=1}^{N_y} \bar{C}^y_{jq} w^b_{iq} + A^y_{j1}\kappa^{yb}_{i1} + A^y_{jN_y}\kappa^{yb}_{iN_y}\right) \\ & - \hat{B}\sum_{p=1}^{N_x}\sum_{q=1}^{N_y} B^x_{ip} A^y_{jq} w^b_{pq} - \alpha C\left(\sum_{q=1}^{N_y} \bar{C}^y_{jq} w^s_{iq} + A^y_{j1}\kappa^{ys}_{i1} + A^y_{jN_y}\kappa^{ys}_{iN_y}\right) \\ & - \alpha\hat{C}\sum_{p=1}^{N_x}\sum_{q=1}^{N_y} B^x_{ip} A^y_{jq} w^s_{pq} - 2B_s\sum_{p=1}^{N_x}\sum_{q=1}^{N_y} B^x_{ip} A^y_{jq} w^b_{pq} \\ & + A_s\left(\sum_{p=1}^{N_x} B^x_{ip} v_{pj} + \sum_{p=1}^{N_x}\sum_{q=1}^{N_y} A^x_{ip} A^y_{jq} u_{pq}\right) - 2\alpha C_s\sum_{p=1}^{N_x}\sum_{q=1}^{N_y} B^x_{ip} A^y_{jq} w^s_{pq} \\ & = I_0\left(\frac{\partial^2 v}{\partial t^2}\right)_{ij} - I_1\sum_{q=1}^{N_y} A^y_{jq}\left(\frac{\partial^2 w^b}{\partial t^2}\right)_{iq} - I_3\sum_{p=1}^{N_y} A^y_{jq}\left(\frac{\partial^2 w^s}{\partial t^2}\right)_{iq} \end{aligned} \qquad (39)$$

Equation (30):

$$\begin{aligned} & B\sum_{p=1}^{N_x} C^x_{ip} u_{pj} + \hat{B}\sum_{p=1}^{N_x}\sum_{q=1}^{N_y} B^x_{ip} A^y_{jq} v_{pq} - D\left(\sum_{p=1}^{N_x} \bar{D}^x_{ip} w^b_{pj} + B^x_{i1}\kappa^{xb}_{1j} + B^x_{iN_x}\kappa^{xb}_{N_x j}\right) \\ & - 2(\hat{D} + 2D_s)\sum_{p=1}^{N_x}\sum_{q=1}^{N_y} B^x_{ip} B^y_{jq} w^b_{pq} - \alpha F\left(\sum_{p=1}^{N_x} \bar{D}^x_{ip} w^s_{pj} + B^x_{i1}\kappa^{xs}_{1j} + B^x_{iN_x}\kappa^{xs}_{N_x j}\right) \\ & - 2\alpha(\hat{F} + 2F_s)\sum_{p=1}^{N_x}\sum_{q=1}^{N_y} B^x_{ip} B^y_{jq} w^s_{pq} + 2B_s\left(\sum_{p=1}^{N_x}\sum_{q=1}^{N_y} A^x_{ip} B^y_{jq} u_{pq}\right. \\ & \left. + \sum_{p=1}^{N_x}\sum_{q=1}^{N_y} B^x_{ip} A^y_{jq} v_{pq}\right) + B\sum_{q=1}^{N_y} C^y_{jq} v_{iq} + \hat{B}\sum_{p=1}^{N_x}\sum_{q=1}^{N_y} A^x_{ip} B^y_{jq} u_{pq} \end{aligned}$$

$$-D\left(\sum_{q=1}^{N_y}\bar{D}^y_{jq}w^b_{iq}+A^y_{j1}\kappa^{yb}_{i1}+A^y_{jN_y}\kappa^{yb}_{iN_y}\right)$$
$$-\alpha F\left(\sum_{q=1}^{N_y}\bar{D}^y_{jq}w^s_{iq}+A^y_{j1}\kappa^{ys}_{i1}+A^y_{jN_y}\kappa^{ys}_{iN_y}\right)$$
$$+k_s\left[\sum_{p=1}^{N_x}B^x_{ip}(w^b_{pj}+w^s_{pj})+\sum_{q=1}^{N_y}B^y_{jq}(w^b_{iq}+w^s_{iq})\right]-k_w(w^b_{ij}+w^s_{ij})$$
$$=\frac{\partial^2}{\partial t^2}\left[I_0(w^b_{ij}+w^s_{ij})+I_1\left(\sum_{p=1}^{N_x}A^x_{ip}u_{pj}+\sum_{q=1}^{N_y}A^y_{jq}v_{iq}\right)\right.$$
$$\left.-I_2\left(\sum_{p=1}^{N_x}B^x_{ip}w^b_{pj}+\sum_{q=1}^{N_y}B^y_{jq}w^b_{iq}\right)-\alpha I_4\left(\sum_{p=1}^{N_x}B^x_{ip}w^s_{pj}+\sum_{q=1}^{N_y}B^y_{jq}w^s_{iq}\right)\right] \quad (40)$$

Equation (31):

$$\alpha\left[C\sum_{p=1}^{N_x}C^x_{ip}u_{pj}+\hat{C}\sum_{p=1}^{N_x}\sum_{q=1}^{N_y}B^x_{ip}A^y_{jq}v_{pq}-F\right.$$
$$\left(\sum_{p=1}^{N_x}\bar{D}^x_{ip}w^b_{pj}+B^x_{i1}\kappa^{xb}_{1j}+B^x_{iN_x}\kappa^{xb}_{N_xj}\right)-2(\hat{F}+2F_s)\sum_{p=1}^{N_x}\sum_{q=1}^{N_y}B^x_{ip}B^y_{jq}w^b_{pq}$$
$$-\alpha H\left(\sum_{p=1}^{N_x}\bar{D}^x_{ip}w^s_{pj}+B^x_{i1}\kappa^{ys}_{1j}+B^x_{iN_x}\kappa^{ys}_{N_xj}\right)-2\alpha(\hat{H}+2H_s)$$
$$\sum_{p=1}^{N_x}\sum_{q=1}^{N_y}B^x_{ip}B^y_{jq}w^s_{pq}+2C_s\left(\sum_{p=1}^{N_x}\sum_{q=1}^{N_y}A^x_{ip}B^y_{jq}u_{pq}+\sum_{p=1}^{N_x}\sum_{q=1}^{N_y}B^x_{ip}A^y_{jq}v_{pq}\right)$$
$$+C\sum_{q=1}^{N_y}C^y_{jq}v_{iq}+\hat{C}\sum_{p=1}^{N_x}\sum_{q=1}^{N_y}A^x_{ip}B^y_{jq}u_{pq}-F\left(\sum_{q=1}^{N_y}\bar{D}^y_{jq}w^b_{iq}+A^y_{j1}\kappa^b_{i1}+A^y_{jN_y}\kappa^b_{iN_y}\right)$$
$$\left.-\alpha H\left(\sum_{q=1}^{N_y}\bar{D}^y_{jq}w^s_{iq}+A^y_{j1}\kappa^{ys}_{i1}+A^y_{jN_y}\kappa^{ys}_{iN_y}\right)\right]+k_s\left[\sum_{p=1}^{N_x}B^x_{ip}(w^b_{pj}+w^s_{pj})\right.$$
$$\left.+\sum_{q=1}^{N_y}B^y_{jq}(w^b_{iq}+w^s_{iq})\right]-k_w(w^b_{ij}+w^s_{ij})$$
$$=\frac{\partial^2}{\partial t^2}\left[I_0(w^b_{ij}+w^s_{ij})+\alpha I_3\left(\sum_{p=1}^{N_x}A^x_{ip}u_{pj}+\sum_{q=1}^{N_y}A^y_{jq}v_{iq}\right)\right.$$
$$\left.-\alpha I_4\left(\sum_{p=1}^{N_x}B^x_{ip}w^b_{pj}+\sum_{q=1}^{N_y}B^y_{jq}w^b_{iq}\right)-\alpha^2 I_6\left(\sum_{p=1}^{N_x}B^x_{ip}w^s_{pj}+\sum_{q=1}^{N_y}B^y_{jq}w^s_{iq}\right)\right], \quad (41)$$

where $\kappa^{\eta\mu}_{ij}=\dfrac{\partial^2 w^\mu}{\partial\eta^2}$ ($\mu=b$ or s and $\eta=x$ or y),

$$\bar{C}^x_{ip}=\sum_{q=2}^{N_x-1}A^x_{iq}B^x_{qp},\ \bar{D}^x_{ip}=\sum_{q=2}^{N_x-1}B^x_{iq}B^x_{qp},\ \bar{C}^y_{jq}=\sum_{q=2}^{N_y-1}A^x_{jp}B^x_{pj},\ \bar{D}^y_{jq}=\sum_{p=2}^{N_y-1}B^x_{jp}B^x_{pq}. \quad (42a–d)$$

Also, the DQ discretized form of the boundary conditions can be obtained in a similar manner. The DQ analogs of the boundary conditions along the edges $\eta=0$ and $\eta=L_\eta$ with $\eta=x$ and y become as follows:

Simply supported edges

At $x=0$ (with $i=1$) and $x=a$ (with $i=N_x$):

$$v_{ij}=0,\ \sum_{p=1}^{N_x}A^x_{ip}u_{pj}=0,\ w^b_{ij}=0,\ w^s_{ij}=0,\ \kappa^{xb}_{ij}=0,$$
$$\kappa^{xs}_{ij}=0 \text{ for } j=1,\ \ldots,\ N_y \quad (43a–f)$$

At $y=0$ (with $j=1$) and $y=b$ (with $j=N_y$):

$$u_{ij}=0,\ \sum_{q=1}^{N_y}A^y_{jq}v_{iq}=0,\ w^b_{ij}=0,\ w^s_{ij}=0,\ \kappa^{yb}_{ij}=0,$$
$$\kappa^{ys}_{ij}=0 \text{ for } i=1,\ \ldots,\ N_x, \quad (44a–f)$$

Clamped edges

$$u_{ij}=0,\ v_{ij}=0,\ w^\mu_{ij}=0,$$
$$\kappa^{\mu\eta}_{ij}-\sum_{n=1}^{N_\eta}\sum_{m=2}^{N_\eta-1}A^\eta_{im}A^\eta_{mn}w^\mu_{nj}=0$$
$$\text{for } \mu=b,\ s \text{ and } \eta=x,y \quad (45a–e)$$

It can be seen that these boundary conditions can easily and directly be implemented into the discretized form of the equations of motion [Equations (38–41)].

Table 1: Constituent material properties of FG plates [11].

Material	Constituent	Properties		
		E (N/m²)	ν	ρ (kg/m³)
Metal	Aluminum (Al)	70×10^9	0.30	2707
Ceramic	Alumina (Al_2O_3)	380×10^9	0.30	3800

Table 2: Comparison study of the nondimensional fundamental frequency parameter ω_1' of simply supported FG plates ($a/b=1$, $K_w=K_s=0$).

	a/h	$p=0$	$p=0.5$	$p=1$	$p=2$	$p=5$
Present (NFSDT)	20	0.0291	0.0247	0.0222	0.0202	0.0191
Present (NHSDT)		0.0291	0.0247	0.0222	0.0202	0.0191
Baferani et al. [15]		0.0291	0.0249	0.0227	0.0209	0.0197
Present (NFSDT)	10	0.1135	0.0963	0.0868	0.0788	0.0743
Present (NHSDT)		0.1135	0.0963	0.0868	0.0787	0.0740
Baferani et al. [15]		0.1134	0.0975	0.0891	0.0819	0.0767
Present (NFSDT)	5	0.4153	0.3542	0.3194	0.2891	0.2701
Present (NHSDT)		0.4154	0.3547	0.3195	0.2880	0.2659
Baferani et al. [15]		0.4154	0.3606	0.3299	0.3016	0.2765

Table 3: Comparison study of the nondimensional fundamental frequency parameter ω_1' of simply supported FG plates ($a/b=1$, $K_w=K_s=100$).

	a/h	$p=0$	$p=0.5$	$p=1$	$p=2$	$p=5$
Present (NFSDT)	20	0.0411	0.0392	0.0384	0.0381	0.0384
Present (NHSDT)		0.0411	0.0392	0.0384	0.0381	0.0383
Baferani et al. [15]		0.0411	0.0395	0.0388	0.0386	0.0388
Present (NFSDT)	10	0.1619	0.1549	0.1518	0.1503	0.1515
Present (NHSDT)		0.1619	0.1549	0.1518	0.1503	0.1513
Baferani et al. [15]		0.1619	0.1563	0.1542	0.1535	0.1543
Present (NFSDT)	5	0.6161	0.5940	0.5830	0.5770	0.5817
Present (NHSDT)		0.6162	0.5942	0.5831	0.5768	0.5807
[Baferani et al. [15]		0.6162	0.6026	0.5978	0.5970	0.5993

Using the harmonic nature of the temporal variation of the displacement components in free vibration motion, subsequently, one obtains a system of eigenvalue equations from which the FG plate natural frequencies and the related mode shapes are obtained [9, 33, 34, 38].

4 Numerical results

In this section, first, the accuracy of the presented formulation for the free vibration of the FG plates is demonstrated by comparing the analytical solution with those of other available results in the open literature. In addition, the convergence behavior and accuracy of the numerical solution (DQM) is investigated. The constituent material properties of FG plates are given in Table 1. The boundary conditions of the plate are specified by the letter symbols; for example, C-S-C-S indicates that the edges $x=0$ and $y=0$ are clamped and the edges $x=a$ and $y=b$ are simply supported, respectively. Also, the following nondimensional parameters are used in this section,

$$K_s=\frac{k_s a^2}{D_m},\ K_w=\frac{k_w a^4}{D_m},\ \omega_i'=\omega_i h\sqrt{\rho_m/E_m},$$
$$\bar{\omega}_i=\omega_i(a^2/h)\sqrt{\rho_m/E_m},\ \hat{\omega}_i=\omega_i(a^2/h)\sqrt{\rho_c/E_c},$$
$$\tilde{\omega}_i=\omega_i(a^2/\pi^2)\sqrt{\rho_c h/D_c}, \tag{46}$$

where $D_m=\dfrac{E_m h^3}{12(1-\nu_m^2)}$ and $D_c=\dfrac{E_c h^3}{12(1-\nu_c^2)}$.

Table 4: Comparison study of the nondimensional fundamental frequency parameter $\bar{\omega}_1$ of simply supported FG plates ($K_w=K_s=0$).

	a/b	a/h	$p=0$	$p=0.5$	$p=1$	$p=2$	$p=5$	$p=10$
Present (NFSDT)	0.5	5	6.7666	5.7576	5.1907	4.7040	4.4154	4.2537
Present (NHSDT)			6.7672	5.7624	5.1912	4.6909	4.3658	4.2010
Tahi and Choi [54]			6.7610	5.7657	5.2016	4.7052	4.3757	4.2058
Present (NFSDT)		10	7.1812	6.0891	5.4875	4.9843	4.7121	4.5562
Present (NHSDT)			7.1813	6.0905	5.4876	4.9801	4.6961	4.5391
Tahi and Choi [54]			7.1746	6.0886	5.4887	4.9833	4.6987	4.5404
Present (NFSDT)		20	7.3003	6.1837	5.5723	5.0649	4.7986	4.6450
Present (NHSDT)			7.3003	6.1841	5.5723	5.0638	4.7943	4.6404
Tahi and Choi [54]			7.2936	6.1805	5.5704	5.0632	4.7943	4.6404
Present (NFSDT)	1	5	10.3835	8.8553	7.9860	7.2270	6.7535	6.4909
Present (NHSDT)			10.3857	8.8665	7.9874	7.1989	6.6465	6.3777
Tahi and Choi [54]			10.3761	8.8764	8.0122	7.2311	6.6678	6.3879
Present (NFSDT)		10	11.3454	9.6274	8.6769	7.8772	7.4349	7.1832
Present (NHSDT)			11.3456	9.6309	8.6771	7.8670	7.3962	7.1418
Tahi and Choi [54]			11.3351	9.6298	8.6824	7.8763	7.4034	7.1453
Present (NFSDT)		20	11.6415	9.8639	8.8879	8.0746	7.6385	7.3912
Present (NHSDT)			11.6414	9.8630	8.8879	8.0774	7.6494	7.4028
Tahi and Choi [54]			11.6307	9.8587	8.8859	8.0749	7.6394	7.3916
Present (NFSDT)	2	5	22.7040	19.4905	17.5983	15.8703	14.6534	13.9898
Present (NHSDT)			22.7255	19.5435	17.6125	15.7711	14.2582	13.5750
Tahi and Choi [54]			22.7045	19.5910	17.7148	15.8953	14.3312	13.6095
Present (NFSDT)		10	27.0664	23.0304	20.7630	18.8159	17.6616	17.0150
Present (NHSDT)			27.0689	23.0497	20.7646	18.7635	17.4631	16.8040
Tahi and Choi [54]			27.0439	23.0629	20.8063	18.8206	17.5028	16.8232
Present (NFSDT)		20	28.7248	24.3564	21.9501	19.9374	18.8483	18.2250
Present (NHSDT)			28.7250	24.3620	21.9502	19.9205	18.7843	18.1564
Tahi and Choi [54]			28.6985	24.3544	21.9548	19.9333	18.7950	18.1616

Table 5: Comparison study of the nondimensional fundamental frequency parameter $\bar{\omega}_1$ of simply supported FG plates on elastic foundation ($K_w=K_s=100$).

	a/b	*a/h*	*p*=0	*p*=0.5	*p*=1	*p*=2	*p*=5	*p*=10
Present (NFSDT)	0.5	5	11.4054	11.2232	11.1510	11.1619	11.3325	11.4457
Present (NHSDT)			11.4057	11.2249	11.1511	11.1592	11.3235	11.4360
Thai and Choi [54]			11.3952	11.2331	11.1780	11.2018	11.3593	11.4558
Present (NFSDT)		10	11.7365	11.5020	11.4243	11.4467	11.6226	11.7113
Present (NHSDT)			11.7366	11.5027	11.4244	11.4451	11.6171	11.7056
Thai and Choi [54]			11.7257	11.4992	11.4270	11.4530	11.6243	11.7093
Present (NFSDT)		20	11.8355	11.5846	11.5044	11.5290	11.7070	11.7904
Present (NHSDT)			11.8355	11.5848	11.5044	11.5285	11.7053	11.7886
Thai and Choi [54]			11.8246	11.5780	11.5005	11.5273	11.7054	11.7886
Present (NFSDT)	1	5	15.4034	14.8508	14.5757	14.4259	14.5428	14.6536
Present (NHSDT)			15.4046	14.8557	14.5763	14.4189	14.5185	14.6276
Thai and Choi [54]			15.3904	14.8757	14.6305	14.5004	14.5843	14.6636
Present (NFSDT)		10	16.1877	15.4890	15.1787	15.0312	15.1501	15.2132
Present (NHSDT)			16.1878	15.4910	15.1788	15.0266	15.1339	15.1964
Thai and Choi [54]			16.1728	15.4895	15.1887	15.0455	15.1497	15.2045
Present (NFSDT)		20	16.4401	15.6928	15.3698	15.2216	15.3447	15.3975
Present (NHSDT)			16.4401	15.6934	15.3698	15.2202	15.3395	15.3921
Thai and Choi [54]			16.4249	15.6851	15.3663	15.2209	15.3414	15.3929
Present (NFSDT)	2	5	28.6587	26.6939	25.5744	24.6816	24.4355	24.4661
Present (NHSDT)			28.6732	26.7225	25.5810	24.6500	24.3121	24.3323
Thai and Choi [54]			28.6467	26.8009	25.7640	24.9077	24.5036	24.4352
Present (NFSDT)		10	32.4172	29.6813	28.2719	27.2373	26.9211	26.7797
Present (NHSDT)			32.4192	29.6952	28.2730	27.2058	26.8085	26.6630
Thai and Choi [54]			32.3893	29.7133	28.3322	27.2931	26.8741	26.6964
Present (NFSDT)		20	33.9181	30.8659	29.3404	28.2560	27.9547	27.7779
Present (NHSDT)			33.9183	30.8702	29.3404	28.2445	27.9131	27.7345
Thai and Choi [54]			33.8869	30.8606	29.3467	28.2628	27.9294	27.7426

Table 6: Comparison study of the nondimensional frequency parameter $\hat{\omega}_i$ of simply supported FG plates (a/b=1, $h/a=0.1$, $K_w=K_s=0$).

			p=0			*p*=1
	$\hat{\omega}_1$	$\hat{\omega}_2$	$\hat{\omega}_3$	$\hat{\omega}_1$	$\hat{\omega}_2$	$\hat{\omega}_3$
Present (NHSDT)	5.7694	13.7650	21.1253	4.4124	10.5592	16.2469
Present (NFSDT)	5.7693	13.7637	21.1207	4.4124	10.5583	16.2440
Zhu and Liew [11]	5.7619	13.7980	21.1045	4.4106	10.6130	16.2867
			p=2			*p*=5
Present (NHSDT)	4.0005	9.5415	14.6430	3.7611	8.8803	13.5194
Present (NFSDT)	4.0057	9.5682	14.7002	3.7808	8.9812	13.7370
Zhu and Liew [11]	4.0059	9.6266	14.7585	3.7806	9.0267	13.7768

There are some research studies that cover the free vibration of the FG plates, and they have interesting examples for comparison, such as those of Zhu and Liew [11], Baferani et al. [15], Reddy [51], Bian et al. [52], Lü et al. [53], and Thai and Choi [54]. Studies more relevant to the present work are chosen for comparison. As a first example, in Tables 2 and 3, the nondimensional fundamental natural frequency parameters of the rectangular simply supported FG plates with and without elastic foundation are compared with those of the higher-order theory of Baferani et al. [15]. Again, as another example, in Tables 4 and 5, a comparison between the nondimensional fundamental natural frequency parameter results of presented method and those obtained by Thai and Choi [54] are prepared for the rectangular simply supported FG plates with and without elastic foundation. The

Table 7: Convergence behavior of the DQM for the first three nondimensional frequency parameters $\bar{\omega}_i$ of FG plates on elastic foundation ($a/b=1$, $h/a=0.2$, $p=1$, $K_w=K_s=100$).

	$N_x=N_y$	C-S-S-S			C-S-C-S		
		$\bar{\omega}_1$	$\bar{\omega}_2$	$\bar{\omega}_3$	$\bar{\omega}_1$	$\bar{\omega}_2$	$\bar{\omega}_3$
NFSDT	9	15.5911	26.1740	27.3872	16.6424	26.7527	29.2401
	11	15.5916	26.1751	27.3938	16.6430	26.7546	29.2646
	17	15.5916	26.1752	27.3936	16.6430	26.7547	29.2639
	19	15.5916	26.1752	27.3936	16.6430	26.7547	29.2639
NHSDT	9	15.5993	26.1861	27.4294	16.6645	26.7724	29.3208
	11	15.6039	26.1897	27.4530	16.6767	26.7810	29.3801
	17	15.6119	26.1951	27.4846	16.6997	26.7944	29.4476
	19	15.6129	26.1958	27.4912	16.7026	26.7961	29.4566
	21	15.6135	26.1961	27.4935	16.7042	26.7970	29.4613
	23	15.6137	26.1963	27.4946	16.7049	26.7974	29.4637

Table 8: Accuracy of the DQM in predicting the first three nondimensional frequency parameters $\tilde{\omega}_i$ of the S-C-S-C FG plates ($a/b=1$, $p=1$, $K_w=K_s=0$).

	$h/a=0.3$			$h/a=0.5$		
	$\tilde{\omega}_1$	$\tilde{\omega}_2$	$\tilde{\omega}_3$	$\tilde{\omega}_1$	$\tilde{\omega}_2$	$\tilde{\omega}_3$
Present (NHSDT)	1.5942	2.6842	3.0311	1.1932	1.9223	2.0649
Malekzadeh [33]	1.5142	2.6522	2.8637	1.1150	1.8354	1.9489

Table 9: Comparison study of the nondimensional fundamental frequency parameter $\bar{\omega}_1$ of the simply supported square FG plates ($a/b=1$, $K_w=K_s=0$).

	BC	a/h	$p=0$	$p=0.5$	$p=1$	$p=2$	$p=5$	$p=10$
Present (NFSDT)	SCSC	5	13.9344	11.9993	10.8865	9.8667	9.1008	8.6500
Present (NHSDT)			13.9815	12.0590	10.9186	9.8229	8.8776	8.4242
Present (NFSDT)		10	16.1675	13.7679	12.4337	11.2915	10.6057	10.2042
Present (NHSDT)			16.1747	13.7827	12.4384	11.2662	10.5020	10.0955
Present (NFSDT)		20	16.9412	14.3674	12.9542	11.7738	11.1343	10.7627
Present (NHSDT)			16.9418	14.3707	12.9546	11.7655	11.1022	10.7286
Present (NFSDT)	SSSC	5	12.0145	10.3014	9.3286	8.4605	7.8593	7.5060
Present (NHSDT)			12.0288	10.3271	9.3381	8.4223	7.7016	7.3440
Present (NFSDT)		10	13.4442	11.4292	10.3146	9.3701	8.8262	8.5087
Present (NHSDT)			13.4460	11.4361	10.3157	9.3541	8.7607	8.4432
Present (NFSDT)		20	13.9052	11.7868	10.6253	9.6581	9.1412	8.8412
Present (NHSDT)			13.9053	11.7885	10.6254	9.6534	9.1232	8.8221

comparison studies in Tables 2–5 are performed for the different values of the material property graded index "p" and the three different values of the length-to-thickness (a/h) ratio. The results of both new first-order shear deformation theory (NFSDT) and new higher-order shear deformation theory (NHSDT) are presented in these tables. A shear correction factor of 5/6 is used for the NFSDT. It can be seen that in all cases, the results of the present formulation are almost the same as those obtained by Baferani et al. [15]. The accuracy of the present formulation is further exhibited by comparing the first three frequency parameters of the simply supported moderately thick FG plates obtained using the NFSDT and the NHSDT with those of the conventional FSDT [11] in Table 6. The results are prepared for the different values of the material property graded index "p", and close agreement between the results of the present theory with those of Zhu and Liew [11] can be observed. It should be mentioned that Zhu and

Table 10: Comparison study of the nondimensional fundamental frequency parameter $\bar{\omega}_1$ of the simply supported square FG plates on elastic foundation ($a/b=1$, $K_w=K_s=100$).

	BC	a/h	$p=0$	$p=0.5$	$p=1$	$p=2$	$p=5$	$p=10$
Present (NFSDT)	SCSC	5	18.1880	17.1657	16.6430	16.2540	16.1021	16.0148
Present (NHSDT)			18.2561	17.2422	16.7026	16.2735	16.0371	15.9581
Present (NFSDT)		10	20.1330	18.6683	17.9461	17.4411	17.2994	17.2019
Present (NHSDT)			20.1445	18.6864	17.9567	17.4305	17.2357	17.1383
Present (NFSDT)		20	20.8430	19.2141	18.4221	17.8858	17.7796	17.7007
Present (NHSDT)			20.8441	19.2175	18.4231	17.8797	17.7546	17.6747
Present (NFSDT)	SSSC	5	16.7001	15.9521	15.5916	15.3645	15.3632	15.3576
Present (NHSDT)			16.7231	15.9820	15.6129	15.3647	15.3166	15.3155
Present (NFSDT)		10	17.9016	16.8955	16.4184	16.1289	16.01400	16.1284
Present (NHSDT)			17.9194	16.9027	16.4218	16.1216	16.1055	16.0936
Present (NFSDT)		20	18.3276	17.2136	16.6980	16.3920	16.4219	16.4188
Present (NHSDT)			18.3280	17.2151	16.6984	16.3889	16.4096	16.4061

Liew [11] conducted the results based on the conventional FSDT using the local Kriging meshless method.

The convergence behavior of the DQM in solving the free vibration equations of the FG plates on elastic foundation based on the present NFSDT and NHSDT is studied in Table 7. For this purpose, the FG plates with two different set of boundary conditions are analyzed, and their first three frequency parameters are presented in Table 7. It is evident that using only the few grid points converged, accurate results are obtained, which demonstrate the high computational efficiency of the DQM. Hereafter, a value of $N_x=N_y=N=19$ is used to report the numerical results for the FG plates. In addition, the accuracy of the DQM is demonstrated by showing its ability in predicting the first three nondimensional frequency parameters of the S-C-S-C FG plates in Table 8. The results are compared with the three-dimensional solution obtained using a semianalytical method by Malekzadeh [33]. The close agreement of the results demonstrates the correctness of the formulation and method of solution.

The accuracy of the present formulation, both NFSDT and NHSDT, is further demonstrated by investigating the free vibration of moderately thick FG plates with and without elastic foundation subjected to some mixed boundary conditions in Tables 9 and 10, respectively. The results are prepared for different values of the material graded index "p", three different values of the thickness-to-length ratio, and two mixed set of boundary conditions.

5 Conclusions

A simple, accurate, and unified four-variable formulation for the free vibration analysis of FG plates is introduced. The transverse shear deformations and rotary inertia effects are included, and the shear correction factors are not necessary for the NHSDT. The only assumption of this formulation, despite the other four-variable theories, is the decomposition of the transverse displacement into bending and shear components. Consequently, some new functions are developed for the in-plane displacement component explanation. This theory is free of the assumption of zero in-plane resultant forces used in developing the other four-variable shear deformation theories and hence has the potential to be used for modeling of the nonlinear FG plate problems. It is shown that new four-variable first- and third-order shear deformation theories, as against five variables in the case of the conventional form of these theories, and also CPT can be easily achieved. The equations of motion and the related boundary conditions for the FG plates on two-parameter elastic foundation are derived using Hamilton's principle. Exact solutions for the simply supported FG plates are extracted. In addition, by extending the application of DQM as an accurate and computationally efficient numerical method, approximate solutions for the FG plates with arbitrary boundary conditions are developed. Comparison studies with the other available two- and three-dimensional solutions in the open literature are performed and excellent agreement is observed. For future studies, extension of this formulation for the nonlinear FG plate problems is suggested.

References

[1] Birman V, Byrd LW. *ASME Appl. Mech. Rev.* 2007, 60, 195–216.
[2] Yang J, Shen HS. *Compos. Struct.* 2001, 54, 497–508.

[3] Hasani Baferani A, Saidi AR, Jomehzadeh E. *Proc. Inst. Mech. Eng. Part C J. Mech. Eng. Sci*. 2011, 225, 526–536.
[4] Cheng ZQ, Kitipornchai S. *ASCE J. Eng. Mech*. 1999, 125, 1293–1297.
[5] Batra RC, Jin J. *J. Sound Vib*. 2005, 282, 509–516.
[6] Yang J, Shen HS. *J. Sound Vib*. 2002, 255, 579–602.
[7] Zhao X, Lee YY, Liew KM. *J. Sound Vib*. 2009, 319, 918–939.
[8] Hosseini-Hashemi S, Rokni Damavandi T, Akhavan H, Omidi M. *Appl. Math. Model*. 2010, 34, 1276–1291.
[9] Malekzadeh P, Alibeygi Beni A. *Compos. Struct*. 2010, 92, 2758–2767.
[10] Hosseini-Hashemi S, Fadaee M, Atashipour SR. *Int. J. Mech. Sci*. 2011, 53, 11–22.
[11] Zhu P, Liew KM. *Compos. Struct*. 2011, 93, 2925–2944.
[12] Cheng ZQ, Batra RC. *J. Sound Vib*. 2000, 229, 879–895.
[13] Ferreira AJM, Batra RC, Roque CMC, Qian LF, Jorge RMN. *Compos. Struct*. 2006, 75, 593–600.
[14] Hosseini-Hashemi S, Fadaee M, Atashipour SR. *Compos. Struct*. 2011, 93, 722–735.
[15] Baferani AH, Saidi AR, Ehteshami H. *Compos. Struct*. 2011, 93, 1842–1853.
[16] Roque CMC, Ferreira AJM, Jorge RMN. *J. Sound Vib*. 2007, 300, 1048–1070.
[17] Shahrjerdi A, Bayat M, Mustapha F, Sapuan SM, Zahari R. *Aust. J. Basic Appl. Sci*. 2010, 4, 893–905.
[18] Benachour A, Tahar HD, Atmane HA, Tounsi A, Ahmed MS. *Compos. Part B Eng*. 2011, 42, 1386–1394.
[19] Mechab I, Mechab B, Benaissa S. *Compos. Part B Eng*. 2013, 45, 748–754.
[20] Qian LF, Batra RC, Chen LM. *Comput. Model Eng. Sci*. 2003, 4, 519–534.
[21] Qian LF, Batra RC, Chen LM. *Compos. Part B Eng*. 2004, 35, 685–697.
[22] Matsunaga H. *Compos. Struct*. 2008, 82, 499–512.
[23] Fares ME, Elmarghany MK, Atta D. *Compos. Struct*. 2009, 91, 296–305.
[24] Talha M, Singh BN. *Appl. Math. Model.* 2010, 34, 3991–4011.
[25] Ait Atmane H, Tounsi A, Mechab I, Bedia EAA. *Int. J. Mech. Mater. Des*. 2010, 6, 113–121.
[26] Neves AMA, Ferreira AJM, Carrera E, Cinefra M, Roque CMC, Jorge RMN, Soares CMM. *Compos. Struct*. 2012, 94, 1814–1825.
[27] Neves AMA, Ferreira AJM, Carrera E, Roque CMC, Cinefra M, Jorge RMN, Soares CMM. *Compos. Part B Eng*. 2012, 43, 711–725.
[28] Brischetto S, Tornabene F, Fantuzzi N, Viola E. *Meccanica* 2016, 51, 2059–2098.
[29] Akavci SS, Tanrikulu AH. *Compos. Part B Eng*. 2015, 83, 203–215.
[30] Fantuzzi N, Tornabene F, Viola E. *Mech. Adv. Mater. Struct*. 2016, 23, 89–107.
[31] Reddy JN. *Trans. ASME J. Appl. Mech*. 1984, 51, 745–752.
[32] Shimpi RP. *AIAA J*. 2002, 40, 137–146.
[33] Malekzadeh P. *Compos. Struct*. 2009, 89, 367–373.
[34] Karami G, Malekzadeh P. *Int. J. Numer. Meth. Eng*. 2003, 56, 847–868.
[35] Bert CW, Malik M. *Appl. Mech. Rev*. 1996, 49, 1–27.
[36] Malekzadeh P. *Compos. Struct*. 2008, 83, 189–200.
[37] Alibeygi Beni A, Malekzadeh P. *Compos. Struct*. 2012, 94, 3215–3222.
[38] Setoodeh AR, Ghorbanzadeh M, Malekzadeh P. *Proc. IME CJ Mech. Eng. Sci*. 2012, 226, 2860–2873.
[39] Tornabene F, Fantuzzi N, Bacciocchi M, Viola E. *Compos. Part B Eng*. 2016, 89, 187–218.
[40] Tornabene F, Fantuzzi N, Viola E, Batra RC. *Compos. Struct*. 2015, 119, 67–89.
[41] Tornabene F, Fantuzzi N, Bacciocchi M. *Compos. Part B Eng*. 2014, 67, 490–509.
[42] Shariyat M, Asemi K. *Compos. Struct*. 2016, 142, 57–70.
[43] Fazzolari FA, Carrera E. *J. Sound Vib*. 2014, 333, 1485–1508.
[44] Fazzolari FA. *Compos. Struct*. 2015, 121, 197–210.
[45] Fazzolari FA. *Compos. Part B Eng*. 2016, 89, 408–423.
[46] Tornabene F, Reddy JN. *J. Indian Inst. Sci*. 2013, 93, 635–688.
[47] Tornabene F, Fantuzzi N, Viola E, Reddy JN. *Compos. Part B Eng*. 2014, 57, 269–296.
[48] So AH, Kuruoglu N. *Thin-Walled Struct*. 2016, 102, 68–79.
[49] Tornabene F, Fantuzzi N, Bacciocchi M. *Fract. Struct. Integr*. 2014, 29, 251–265.
[50] Tornabene F, Fantuzzi N, Ubertini F, Viola E. *Appl. Mech. Rev*. 2015, 67, 020801–020855.
[51] Reddy JN. *Int. J. Numer. Methods Eng*. 2000, 47, 663–684.
[52] Bian ZG, Chen WQ, Lim CW, Zhang N. *Int. J. Solids Struct*. 2005, 42, 6433–6456.
[53] Lü CF, Lim CW, Chen WQ. *Int. J. Numer. Methods Eng*. 2009, 79, 25–44.
[54] Thai HT, Choi DH. *Compos. Part B Eng*. 2012, 43, 2335–2347.